Isolation and Characterization of Retinal Microglia In Royal College of Surgeons Rat

Anil M. Shivaram

YALE UNIVERSITY

2003

Isolation and Characterization of Retinal Microglia in Royal College of Surgeons Rat

A Thesis Submitted to the
Yale University School of Medicine
in Partial Fulfillment of the Requirements for the
Degree of Doctor of Medicine

By

Anil M. Shivaram

2003

Isolation and Characterization of Retinal Microglia in Royal College of Surgeons Rat

Anil M. Shivaram, Nobuo Jo, Yoshiko Usui, Guey-Shuang Wu, and Narsing A. Rao. Doheny Eye Institute, University of Southern California, School of Medicine, Los Angeles, CA. (Sponsored by Ron A. Adelman, Department of Ophthalmology and Visual Sciences, Yale University School of Medicine, New Haven, CT)

PURPOSE: To demonstrate that retinal microglial migration from the ganglion cell layer (GCL) to the photoreceptor later (PRL) in the black-eyed, pigmented Royal College of Surgeons (RCS) p+ rat with inherited retinal dystrophy differs from microglial migration in the pink-eyed RCS strain.

METHODS: Two separate techniques of identifying retinal microglia as they migrated from the ganglion cell layer (GCL) to the photoreceptor layer (PRL) were employed. A fluorescent, lipophilic dye, 4Di-10ASP, was injected into the superficial superior colliculus of newborn (postnatal day 1) RCS p+ pups. This dye, which is retrogradely transported to ganglion cells of the inner retina, is then phagocytosed by resident retinal microglia as the ganglion cells undergo normal programmed cell death. Fluorescent microglial migration was followed by imaging retinal sections from postnatal days 21, 31, 45, and 60. Similarly, retinal sections from enucleated eyes of RCS p+ pups on postnatal days 21, 31, and 45 were stained for the macrophage/microglia marker, CD11b (OX42), using indirect immunohistochemistry techniques.

RESULTS: Retinal microglia identified through labeling with 4Di-10ASP were found to have reached the photoreceptor layer (PRL) by postnatal day 31. Similarly, microglia staining positive for OX42 were also found to have reached the PRL by postnatal day 31. However, in both methods, no microglia were visible within the photoreceptor layer at postnatal day 21.

CONCLUSIONS: This experiment was designed to use different methodologies aimed at identifying retinal microglia to ascertain if there was a difference in the time course of microglial migration between two strains of rats with inherited retinal dystrophy, the black-eyed RCS p+ and the pink-eyed RCS variant. From prior studies, it has been shown that retinal microglia are attracted to the photoreceptor layer as photoreceptor outer segment debris accumulates in rats with this form of inherited retinal dystrophy. Compared to the previously studied pink-eyed RCS strain, the pigmented RCS p+ rat shows a slowing of microglial migration by approximately ten days.

ACKNOWLEDGEMENTS

I would like to extend my sincerest thanks to Narsing Rao for his intellectual inspiration and for allowing me the opportunity to spend some time researching on the "Left" Coast; Guey-Shuang (Kay) Wu for her readiness to answer any and all of my questions with amazing detail; Yoshiko Usui for helping me find my way around in a new place and introducing me to close-by fish tacos for those late nights in lab; Nobuo Jo for his proficiency in the art of immunostaining; Robert See for walking me through my first canthotomy/axotomy and always being there; Sunil Shivaram, Amisha Gupta, and Rajan Shivaram for giving me a home in Southern California for all those months; Lisa P. Roy for never complaining (much) that her other half was thousands of miles away; The Office of Student Research at Yale University School of Medicine for providing me with the funding that made my trip out West possible; Richard Rohrbaugh and Jennifer Dolan for allowing me a little extra time to finish writing up this thesis; and finally, my family, Mysore, Prema, and Anju Shivaram, for always being supportive, loving and a perpetual source of strength.

TABLE OF CONTENTS

INTRODUCTION

Since the early 1960's, the study of retinal degenerative disorders has been rooted in the understanding of cellular movements and interactions based upon animal models (1). These animal constructs have shed much light on correlative human diseases involving the eye. One particular animal model, the RCS rat (named in honor of its original source, the Royal College of Surgeons) has been studied extensively over the past forty years, providing us with some of the biological insight we hold today regarding diseases such as retinitis pigmentosa (RP) and age-related macular degeneration (AMD).

Specifically, retinitis pigmentosa (RP) represents a variegated family of inherited retinal degenerations where the loss of vision results from initial destruction of rod photoreceptors, frequently due to a mutation specific to this photoreceptor cell type (2). The death of rod photoreceptors, largely responsible for low-light/night vision, is subsequently followed by death of the remaining cone photoreceptor cell type (3). This pattern of low acuity to high acuity photoreceptor loss in human disease is similarly represented in the RCS rat model and has served as the source for two putative mechanisms of disease.

The first theory postulates that photoreceptor apoptosis is the result of defective retinal pigment epithelium (RPE) (4). The RPE layer of cells is functionally responsible for the digestion of photoreceptor debris as it accumulates. In those RCS rats with retinal dystrophy, a mutant gene known as *rdy* has been identified and recently uncovered to be a deletion in the receptor tyrosine kinase gene *MERTK* (5, 6). RCS rats lacking the *MERTK* gene have retinal pigment epithelium that is unable to phagocytose outer segment photoreceptor debris as it accumulates. Similarly, human patients with this

deletion of the receptor tyrosine kinase gene have been found to develop a severe form of retinitis pigmentosa (7). Accumulation of unphagocytosed outer segment photoreceptor debris is additionally thought to separate the photoreceptor cells from other cell types it requires for maintenance and nutrition. Recently, however, some doubt has been cast upon this hypothesis with data to support "rescue" of RCS photoreceptors through the use of different compounds such as basic fibroblast growth factor (bFGF) and ciliary neurotrophic factor (CNTF), despite the presence of debris accumulation (8, 9).

A second theory, more interrelated rather than mutually exclusive, proposes that photoreceptor cell death is linked to damage sustained by invading retinal microglia (10). These cells, which are bone marrow-derived, invade the central nervous system (CNS) during embryogenesis while the blood-brain barrier is still open and take up residence within the retina. Until recently, their role has been limited to that of a phagocytic cell – digesting cellular remnants. They are thought to be signaled by neuronal cell death and are known to migrate to damaged areas of brain. Additionally, retinal microglia have also been found to cause "collateral damage" to cell types surrounding dying neurons through their release of reactive oxygen species, peroxynitrite, tumor necrosis factor (TNFα), and other proinflammatory cytokines (11, 12) These implications that retinal microglia are involved in adjacent neuronal cell injury holds particular promise in its ability to explain the low acuity to high acuity photoreceptor loss described earlier. Moreover, subsequent studies of retinal microglia have determined that they may also serve as antigen-presenting cells (APCs) (13). As such, this bone marrow-derived cell type has been the subject of much research as a major player in retinal cell death. Retinal microglia and their migration to areas of damaged retina have also been a focus of

potential therapeutic intervention. It has been shown that injection of microglia inhibition factor (MIF) results in a lack of both microglia chemotaxis and photoreceptor death (14). Retinal microglia, therefore, represent a highly charged area of study with questions that remain regarding what causes their migration and how such migration might be slowed, modified, or even eliminated to avoid subsequent disease.

It is important to note that while much focus has been placed on the role of retinal microglia as a culprit in certain types of inherited retinal dystrophy, dysfunction involving the retinal pigment epithelium is still considered an active area of interest. Experiments targeting RPE as the source of retinal degeneration have also provided encouraging results. For example, it has been shown using the RCS rat model that implantation of human fetal retinal pigment epithelium into the subretinal space results in photoreceptor salvage (15). Thus, there exist two foci of study within the RCS rat population -- the retinal pigment epithelium (RPE) and retinal microglia. Given the experimental data generated involving each of these targets, many have argued that retinal degeneration in the RCS rat model likely involves both mechanisms with RPE dysfunction initiating a cascade of events (e.g., photoreceptor debris accumulation from a lack of phagocytosis and subsequent microglial chemotaxis from this debris) and retinal microglia (MG) furthering the damaging cascade through the release of inflammatory mediators and toxic species.

The RCS Rat Model

Understanding the progression of research in the field of retinal microglia and retinal degeneration requires a brief history of the creation and use of this animal model. The RCS rat model, a cornerstone in retinal degeneration research, was initially linked to

RP in humans through the similarity of rhodopsin overproduction and the development of abnormal lamellar membranes between rod outer segments and the RPE. In this animal with inherited retinal dystrophy, it was noted that the photoreceptors reached nearly adult form and electroretinogram (ERG) function prior to degeneration, which began in the third postnatal week. Through a study of serial light micrographs from RCS rat retina, a timeline of photoreceptor damage was developed. Still used today as an indicator of the time course of photoreceptor loss in the RCS rat, at postnatal day 20 (p20) outer segment debris membranes are described as accumulating at the surface of the RPE layer. At postnatal day 32 (p32), the outer segment zone has become a disorganized debris-filled area with multiple photoreceptor nuclei degenerating. Finally, by postnatal day 55 (p55), there is disappearance of the majority of photoreceptor nuclei and rhodopsin with the continued presence of a debris zone (16). Interestingly, ten months after photoreceptor degeneration, these rats were still able to respond to some visual stimuli, likely the result of a few remaining photoreceptors still connected to the inner retina. The most profound relationship uncovered from early studies with the RCS model, as noted earlier, was the correlation between the accumulation of outer segment debris from the photoreceptors and the failure of RPE cells to phagocytose them. Also of note, these initial studies showed that when dystrophic rats were raised in darkness, the rate of photoreceptor degeneration was decreased. This finding that the expression of a genetic disorder could be environmentally altered contributed to the some of the experimental therapeutic measures used on patients with early forms of retinitis pigmentosa (17). However, it was the discovery of a link between RPE dysfunction and outer segment debris accumulation

that would become much of the subsequent focus within the field of retinal degeneration research.

Early genetic studies by Bourne and Grüneberg, who discovered inherited retinal dystrophy in the rat, determined the disorder to be autosomal recessive with resulting progressive loss of photoreceptor cells starting in the third postnatal week (18). Since this discovery, several strains of rats with inherited retinal dystrophy have been developed, but the most widely used and studies continues to be derived from the inbred RCS line developed by Sidman (19). The development of congenic strains (genetically identical except for a particular genetic locus) from the original inbred strain of the RCS rat began in the late 1960s with the eventual development of two distinct classes of the RCS animal: the RCS p/+ (black-eyed strain) and the pink-eyed RCS p/p, with each strain being homozygous for the retinal dystrophy gene (*rdy/rdy*) (20).

Retinal Microglia

Microglia were first documented in the early part of the 20th century by Nissl, who described a population of cells found in pathologic brain material that were somewhat elongated and "rod-shaped" (21). He labeled these cells as participants in neurodegenerative disease, possessing both phagocytic and migratory capabilities similar to blood-borne leukocytes. These cells, initially characterized in brain, were subsequently found by Ramon y Cajal to migrate to areas of neuron degeneration for the purpose of phagocytosis (22). The term itself, "microglia," was coined in 1932 by del Rio-Hortega, who upon staining both normal and damaged tissue, was able to

characterize microglia into a "resting" type (ramified) and an "activated" type (amoeboid) (23).

Similar to the heavily studied brain microglia, retinal microglia have been characterized in much the same way. They are thought to be marrow-derived cells which invade the retina during development and, similar to brain microglia, establish themselves as a resting cell population through the entire retina. This cell type has been characterized morphologically with the similar existence of both a quiescent, ramified cell type and an amoeboid activated cell type within the retina. Additionally, retinal microglia have been identified through enzyme histochemistry since they contain high concentrations of nucleoside diphosphatase (NDPase) and thiaminepyrophosphatase (TTPase), making it possible to distinguish them from neuroglial Müller cells. Moreover, in their role as retinal "macrophages," they have been shown to respond with increased enzymatic activity after optic nerve transection in rabbit models. The retinal microglia that respond been found to be the only cell type involved in phagocytosis of ganglion cell debris in the axotomized retina (24)

The advent of immunohistochemical labeling with the use of monoclonal antibodies for macrophage markers has allowed for further characterization of retinal microglia (MG). Lending more credence to the theory that these cells are marrow-derived, retinal microglia in the rat have been shown to stain positively for CD11b (OX42), anti-monocyte-macrophage (ED1), and MHC Class II (OX6), also implicating this cell type as a probable antigen-presenting cell (25). Within the rat retina, Zhang et al have demonstrated that retinal microglia express macrophage markers such as OX42 in sufficient quantity to be able to identify their presence within different layers. However,

Rao et al have noted that in rat studies involving inflammatory processes in the eye (such as autoimmune uveoretinitis), activated retinal microglia could not be easily distinguished from other invading macrophages. Yet, the study of the RCS rat model is not complicated by a pronounced inflammatory response recruiting non-microglia macrophages as in the study of microglia in experimental autoimmune uveoretinitis (26).

Developmentally, it is thought that the infiltration of these originally marrow-derived microglia coincides with the late embryonic/ early postnatal maturation of the retina. During this period when roughly 35% of the ganglion cell population undergoes programmed cell death, it has been postulated that this episode may serve as the trigger for the influx of the eventual resident retinal microglia (26). These dying ganglion cells, which possess processes extending to the superior colliculus and are homogenously scattered throughout the retina, provide a convincing explanation for the uniform presence of retinal microglia throughout the developed retina. As ganglion cells undergo programmed cell death and degrade, this cell death triggers the influx of cells responsible for phagocytosing the cellular debris. Once the blood-brain barrier matures, those phagocytic cells triggered to migrate through ganglion cell death then take up permanent residence within the retina.

Using a technique that takes advantage of this programmed death of roughly one-third of the ganglion cell layer (GCL) population, Thanos et al have demonstrated that retinal microglia can be labeled by the injection of a lipophilic, fluorescent dye (4Di-10ASP) into the superior colliculus of rat brain. This fluorescent dye then retrogradely labels (by day 5) the ganglion cells which possess axons that project to the initially labeled structure (27). As some of these ganglion cells dye, their now fluorescent debris

is phagocytosed by microglial cells, thereby providing a means for identifying this cell type as it takes up residence within the retina. Applying this dye technique to the RCS rat, has allowed for the progressive study of the movement of labeled retinal microglia as outer segment debris accumulates due to the defective function of the retinal pigment epithelium (RPE). Using the pink-eyed strain of RCS rat, Thanos et al injected the lipophilic dye into the superior colliculus of newborn RCS pups (postnatal day 0 or P0). Following the progress of retinal microglia as they migrated from the decaying ganglion cell layer (GCL) to the photoreceptor layer (PRL), Thanos et al determined at postnatal day 21 (P21) microglia perikarya were visible within the PRL. As it was noted in their experiment, even at postnatal day 14 (P14), microglia in the ganglion cell layer were described as already having "long processes with endfeet" extending towards the PRL. This finding led to their conclusion that some microglial chemotactic signal must exist as structural changes within the PRL are known to occur only by postnatal day 20 (P20).

The results obtained by Thanos et al through a novel method of retinal microglia fluorescent labeling, however, were specific to the pink-eyed strain of RCS rat. As noted earlier, the rate of photoreceptor degeneration between the pink-eyed RCS rat and the black-eyed RCS p+ rat strain differs. LaVail et al effectively demonstrated through a serial study of both strains that the pigmented RCS p+ rat has a slowed rate of PRL degeneration of approximately ten days compared to that of the pink-eyed strain with no difference in rhodopsin accumulation between the two. While Thanos et al have demonstrated that retinal microglia reach the photoreceptor layer in the pink-eyed RCS animal by P21, no data exist regarding the black-eyed RCS p+ animal – a model potentially more analogous to humans due to the presence of pigment.

STATEMENT OF PURPOSE AND HYPOTHESIS

The purpose of this work is to demonstrate that retinal microglial migration in the black-eyed, pigmented RCS p+ rat does, in fact, differ from the migration timeline noted in the pink-eyed strain. As photoreceptor degeneration in the RCS p+ strain is slowed compared to the its pink-eyed relative, we have shown that retinal microglia in the RCS p+ strain take a longer period of time to migrate from the ganglion cell layer (GCL) to the photoreceptor layer (PRL). Additionally, this progressive migration of retinal microglia to the PRL was documented through immunohistochemical staining with the OX42 antibody to corroborate this difference in migration between the RCS strains.

METHODS

All animals used for the following experiments were maintained and treated in accordance with the ARVO Statement for the Use of Animals in Ophthalmic and Vision Research.

Microglia Isolation and Culture

The methods used to isolate retinal microglia from rat pups were originally adapted from recently published protocols for isolating microglia from adult monkey and human brains (29, 30, 31). For the purpose of practicing microglia isolation techniques and staining using the OX42 antibody, ten newborn (P7) Long-Evans pups from Charles River (Wilmington, MA) were sacrificed. The eyes were enucleated and hemisected with the lens and vitreous removed. The retina was removed taking care to avoid contamination from the pigment epithelium. The removed retinas were subsequently

rinsed with phosphate buffer solution (PBS) to remove any contaminating blood and then minced with sterile surgical scalpel into small fragments (< $2mm^3$). The retina fragments were placed in Dulbecco's modified Eagle's medium (DMEM; Gibco, Grand Island, NY) which contained 10% fetal bovine serum (FBS; Atlanta Biologicals, Norcross, GA) and 1% penicillin-streptomycin (Gibco). Retina fragments were transferred into a 50 ml centrifuge tube filled with 10ml per 1g weight tissue containing 0.05% trypsin in 0.53 mM EDTA (Gibco). An autoclaved stir bar was placed in the solution and the tube containing the cell suspension was incubated in a water bath at 37°C on a magnetic plate stirrer for 30 minutes.

After this time period had elapsed, the cell suspension was diluted with 10 ml DMEM with 10% FBS (DMEM-FBS) to terminate trypsinization. The cell suspension was gently triturated using a wide-mouth 10 ml pipette and centrifuged at 275*g* for seven minutes. The supernatant was aspirated and the cell pellet resuspended in culture medium. The solution was filtered through a 100 µm nylon mesh placed in a sterile 50 ml centrifuge tube. After filtration, the cell suspension was centrifuged once more at 275*g* for seven minutes and the cell pellet was taken up in a Percoll solution (Amersham Pharmacia Biotech, Piscataway, NJ) with a density of 1.03 g/ml. On top of this solution, 6ml of myelin-gradient buffer (0.78 g/l $NaH_2PO_4 \bullet H_20$, adjusted to pH 7.4 with 3.56 g/l $Na_2HPO_4 \bullet 2H_20$, adding 8.0 g/l NaCl; 0.4 g/l KCl; 2.0 g/l glucose and 0.2% bovine serum albumin (BSA, Organon Technika, The Netherlands) was carefully layered. The gradient was centrifuged at 950*g* for 20 minutes without brakes. The cell debris/myelin layer was gently aspirated with a 10ml pipet and the pellet resuspended and centrifuged at 275*g* for seven minutes.

After supernatant removal, the pellet was resuspended with 5 ml of NH_4Cl (0.155 N) and $KHCO_3$ (0.001 N) solution containing 0.5 ml BSA and kept on ice for fifteen minutes for lysis of contaminating erythrocytes. After this period, the culture medium was added to a total volume of 25 ml and the suspension was centrifuged at 275*g* for seven minutes. The resuspended pellet was taken up in a 50 ml centrifuge tube with 10 ml cell culture medium (DMEM-FBS) and replated directly in 75 cm^2 uncoated tissue culture flasks with 1ng/ml murine granulocyte-macrophage colony stimulating factor (GM-CSF; SIGMA, St. Louis, MO). For purification purposes, the cells were incubated with Ca^{2+}-Mg^{2+} -free Hanks' balanced salt solution (HBSS; SIGMA) containing 0.2% EDTA and 5% FBS for one hour at 4°C and detached by vigorous pipetting.

The resulting cell suspensions were placed in plastic flasks for 30 minutes at 37°C to allow for adherence. Then, those cells that were either still suspended or loosely adherent were removed by gentle shaking of the tissue culture flasks at room temperature. The flasks were incubated in a humidified incubator at 37°C pulsed with an atmosphere of 5% CO_2 and 95% air. The cells were allowed to grow for at least three days and then were replenished with additional medium. Cell cultures were visualized under phase contrast microscopy prior to detachment by vigorous pipetting for subsequent OX42 immunostaining.

In addition, a fluorescence activated cell sorting (FACS) technique was also used to achieve a higher degree of microglial purity in the sample. Since this method met with mixed results, it will not be expanded upon in this study.

Characterization of Microglia in Culture

For the purpose of practicing staining of retinal microglia with OX42 antibody (OX42; Serotec, Oxford, England, UK), cells were detached from tissue culture flasks by vigorous pipetting and plated onto chamber slides (Laboratory-Tek; Nunc, Naperville, IL) and given two days to grow at 37°C in the humidified incubator. The chamber slides were then washed with 0.01 M PBS (pH 7.4) five times. Slides were air dried for two hours and then fixed in acetone at 4°C for five minutes. After washing with PBS three times for five minutes each, slides were incubated (at room temperature) for twenty minutes with 0.3% H_2O_2/PBS solution and then washed again with PBS solution.

Slides were then incubated at room temperature with 1% rabbit serum (diluted from rabbit serum, non-immunized; DAKO) for twenty minutes. Slides were drained and excess serum solution was wiped off. Primary CD11b antibody (OX42; Serotec) was added at a 1:200 dilution (diluted in 0.01M PBS) for each sample, covered and incubated overnight. Slides were then washed four times with PBS for four minutes per wash. Incubation with the secondary antibody(Vector, Burlingame, CA), biotinylated antibody to goat IgG (made in rabbit) at 1:200 dilution. After four washings with PBS for four minutes each, ABC reagents were prepared from the standard ABC kit (Vector). Incubation took place with ABC reagents for 45 minutes at room temperature. Following four PBS washes, substrate solution was prepared by dissolving one tablet of 3-amino-9-ethyl-carbazole (SIGMA) to 2.5 ml N, N-dimethylformamide (DMF). 2.5 ml of AEC/DMF was added to 47.5 ml of 50 mM acetate buffer (pH 5) while continuously mixing. Then 25 µl of 30% H_2O_2 was added immediately prior to use and then filtered through a 0.2 µ filter.

After the addition of the substrate, slides were watched under a light microscope to detect color development (time less than five minutes). The reaction was stopped by washing with tap water and a counterstain was applied using modified Mayer's reagent for one minute. Following a tap water wash for three minutes, the slides were covered with Glycergel (DAKO) and visualized by light microscopy. Of note, negative controls were incubated with PBS in lieu of the primary antibody.

Labeling with Lipophilic Dye of RCS p+ animal

Twelve newborn RCS p+ pups were used for the purpose of this study. On postnatal day 1 (P1), the pups were anesthetized and a skin overlying the superior colliculus was opened with a flap incision. An opening was made in the skull to expose the brain and small crystals of the fluorescent dye 4Di-10ASP, N-4-4-(4-didecylaminostyryl)-N-methylpyridinium iodide, were inserted into the superior colliculus. The skin flap was then closed by suture and the pups replaced as a litter to the mother. The pups were closely followed after the procedure to ensure that the mother would continue to rear. Additionally, the father was removed from the cage to minimize cage crowding and possible post-operative rejection.

The pups were then removed at the following postnatal dates: P21, P31, P45, and P60. Animals from each of these dates were sacrificed with their eyes enucleated, washed in PBS (to minimize erythrocyte contamination), lens and vitreous removed, placed in OCT compound (Tissue-Tek/Sakura, Torrance, CA), frozen using liquid nitrogen, and placed at -70°C for storage. The frozen samples were subsequently cut into 20-25 μm sections using a mechanical cryostat and examined for fluorescence (maximum

emission at 563 nm) under confocal laser scanning microscopy (Carl Zeiss, Oberkochen, Germany).

Indirect Immunohistochemical Staining of RCS p+ animal

RCS p+ pups were also used for a portion of the study involving microglia immunostaining with monoclonal antibodies to rat CD11b (OX42). Adhering to the same timeline used for the superior colliculus injection (SCI) of 4Di-10ASP, RCS p+ pups were sacrificed on the following postnatal dates: P21, P31, P45, and P60. Their eyes were enucleated, lens and vitreous removed, washed in PBS, placed in OCT compound, frozen using liquid nitrogen, and stored at -70°C. Frozen samples were then cut consecutively into 20-25 µm sections with a mechanical cryostat with two sections per frosted slide.

Slides were allowed to dry at room temperature for four hours and then circled using a PAP PEN. Sections were then fixed with freshly prepared 4% paraformaldehyde (PFA) for seven minutes. Following four PBS washes of five minutes each, a blocking buffer was added of 2% horse serum (SIGMA) with 1% BSA in PBS for twenty minutes. The blocking agent was removed by suction pipet with no subsequent wash. The primary mouse anti-rat CD11b antibody (OX42; Serotec) was added using a 1:50 dilution. The slides were allowed to incubate at room temperature with the primary antibody. Sections used as for negative control were incubated with PBS in lieu of the OX42 antibody.

After 36 hours, the sections were washed four times with PBS for five minutes each and the secondary antibody, horse anti-mouse IgG biotin, was added at a dilution of 1:100 for one hour. Following four washes with PBS for five minutes, streptavidin – Texas Red (Vector) was added at a 1:50 dilution and left for one hour. The sections were

again washed four times with PBS for five minutes each cycle and then mounted using fluorescence mounting medium (Vector). Sections were covered until visualization using confocal laser scanning microscopy (Carl Zeiss, Oberkochen, Germany).

H&E Preparation

Four RCS p+ pups were sacrificed with subsequent enucleation in accordance with the postnatal timeline: P11, P21, P31, P45, and P60. Eyes from each postnatal time period were sectioned and underwent H&E staining for analysis by light microscopy. The remaining eyes were prepared for EM by a corneal incision, instillation of 1/2 strength Karnosky's fixative for five minutes, removal of fixative, lens extraction, and storage in fixative at 4°C. Additionally, three Long-Evans pups of identical postnatal age to the RCS p+ group (P11, P21, P31, P60) were sacrificed, enucleated, and sectioned for H&E staining as a non-dystrophic control for the RCS p+ animal.

Statement of Academic Honesty

I was involved with this project from June 2002 through January 2003 and was responsible for the techniques used for microglia isolation and subsequent staining and visualization of both isolated microglia and RCS p+ frozen sections. In addition, two research fellows at the Doheny Eye Institute (DEI) were heavily involved with this work. Yoshiko Usui was responsible for perfecting the technique of superior colliculus injection (SCI) with the fluorescent dye (4Di-10ASP) and assisting me with the use of the confocal microscope. Nobuo Jo was the individual responsible for obtaining the confocal images from the fluorescent dye staining. This work was performed under the supervision of Guey-Shuang Wu, Ph.D and Narsing A. Rao, M.D.

RESULTS

Isolation of Microglia

Following three days of incubation after the microglia isolation procedure, two major cell morphologies were noted using phase contrast microscopy (Fig. 1). Cell types were either round or amoeboid ("activated" state) or slender with long processes ("quiescent" state). The cells with processes were the most adherent to the tissue culture flask and were not easily removable despite vigorous pipetting. Following the purification procedure, the majority of cell types visible were of the rounded or amoeboid shape.

FIGURE 1. Phase contrast micrograph of microglia cell cultures at day 3 from newborn Long-Evans (LE) rats (GM-CSF supplemented medium) with both "activated" or amoeboid cells and quiescent cells visible with slender processes. Magnification, x100.

After transfer to chamber slides, indirect immunohistochemical analysis of the cell types recovered with the antibody to CD11b (OX42), revealed positive staining of individual cell types (Fig. 2). The cells clearly labeled with the antibody demonstrated a tear-drop shape with several small processes. The negative control, where PBS was substitute for the primary antibody, showed no significant staining (Fig. 3).

FIGURE 2. Light photomicrographs of OX42 positive cells showing ramified microglia with short processes. Magnification x100.

FIGURE 3. Light photomicrograph indicating lack of staining using negative control (PBS) as primary antibody. Magnification x100.

H&E Sections of RCS p+ and Long-Evans (LE) control animals

As a method of comparing gross retinal changes in the RCS p+ animal to a non-dystrophic control (Long-Evans), H&E stains from postnatal dates of P11 through P60 demonstrated the serial accumulation of outer segment debris in the PRL. In comparing the stains from postnatal dates 11 and 21, mild accumulation of segment debris begins to be visible by P21. Note that the relative size of the outer nuclear layer in both RCS p+ and Long-Evans (LE) controls are similar (Fig. 4).

Subsequent stains from P31 and 45 revealed additional debris accumulation as the photoreceptor layer has taken on a less coherent, almost "fuzzy" form compared to the discretely layered LE control (Fig. 5). Photoreceptor degeneration which becomes markedly pronounced when comparing the P21 and P31 RCS p+ sections. At higher magnification, numerous photoreceptor nuclei have degenerated. As a result of this degeneration and loss, the outer nuclear layer (ONL) is notably thinned in comparing the RCS p+ P31 to the Long-Evans P31 control. ONL thinning progresses as the RCS p+ P45 section shrinks by more then half of the thickness from P31 as photoreceptor nuclei degenerate and outer segment debris accumulates. Finally, by P60 in the RCS p+ section, photoreceptor nuclei are no longer visible under high magnification. However, a large amount of outer segment debris remains (Fig. 6).

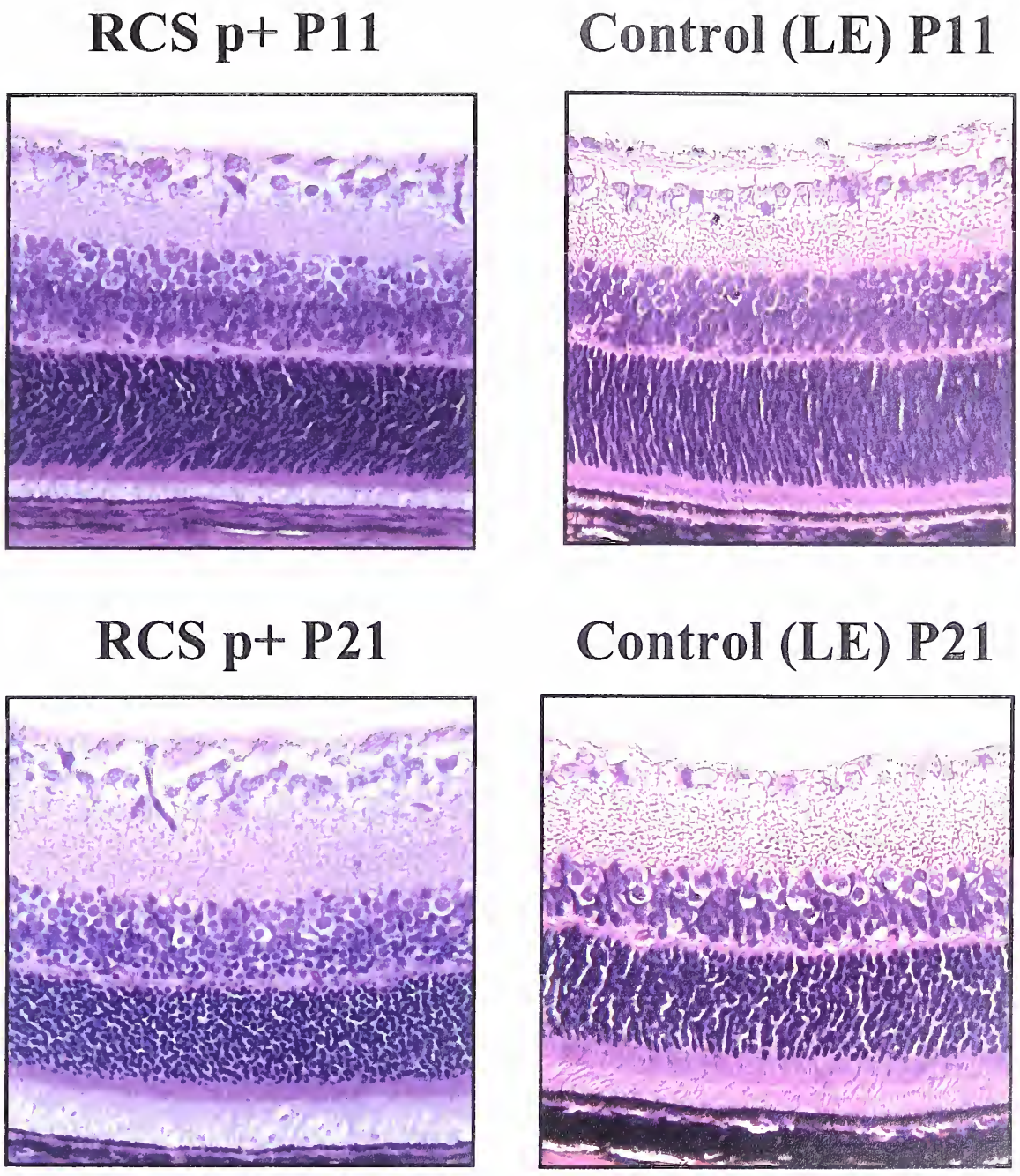

FIGURE 4. H&E sections of RCS p+ and Long-Evans (LE) control at postnatal dates P11 and P21 showing accumulation of outer segment debris at the surface of the retinal pigment epithelium (RPE) by P21 in the RCS p+ animal. Note the lack of debris accumulation in the Long-Evans (LE) control.

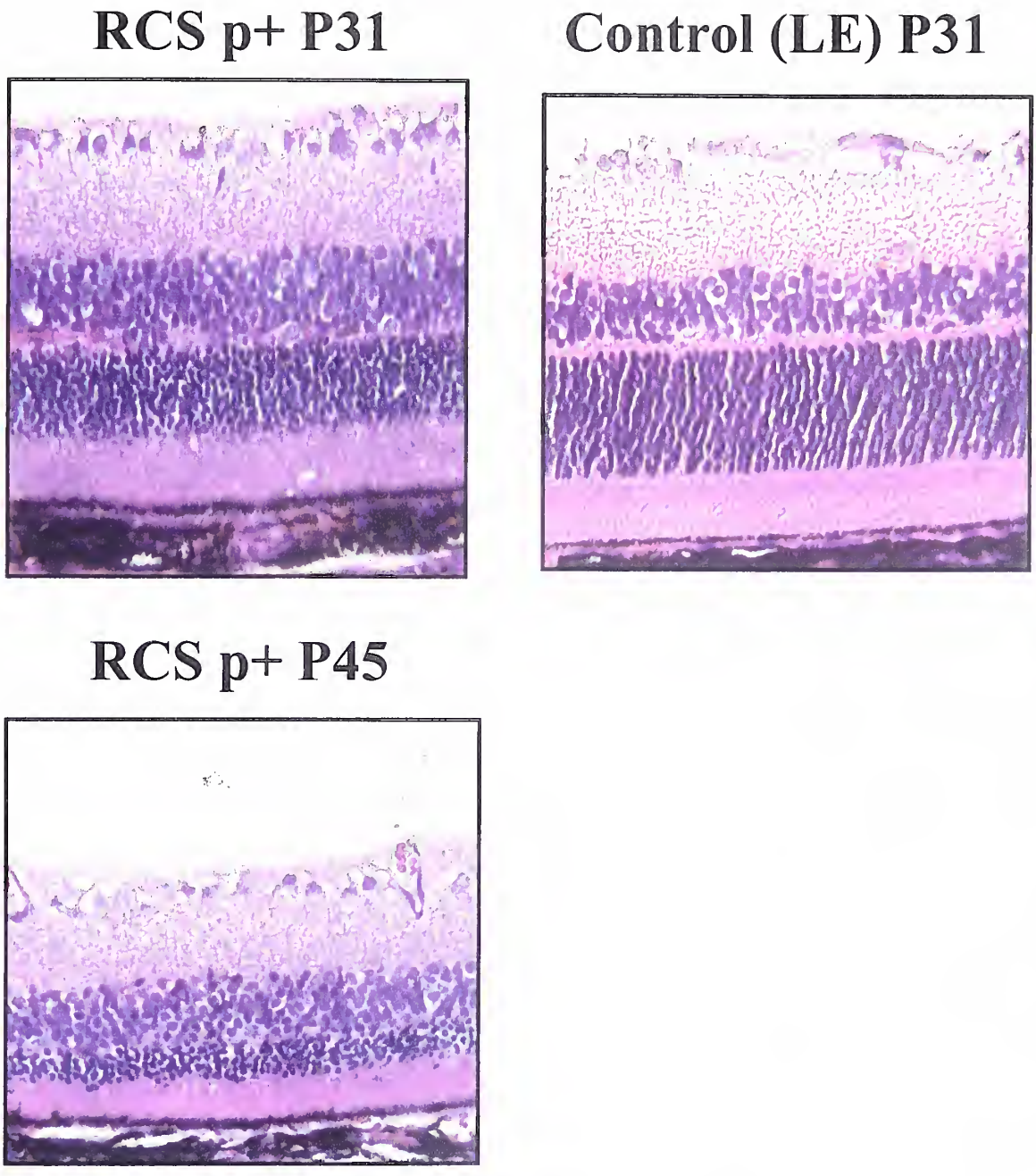

FIGURE 5. H&E sections of RCS p+ and Long-Evans (LE) control at postnatal dates P31 and 45 showing that by P31 the outer segment area has become a disorganized zone of debris in the RCS p+ animal compared to the non-dystrophic Long-Evans control. Higher magnification reveals many photoreceptor nuclei degenerating. As photoreceptor nuclei degenerate and disappear, note the thinning of outer nuclear layer (ONL) by P45.

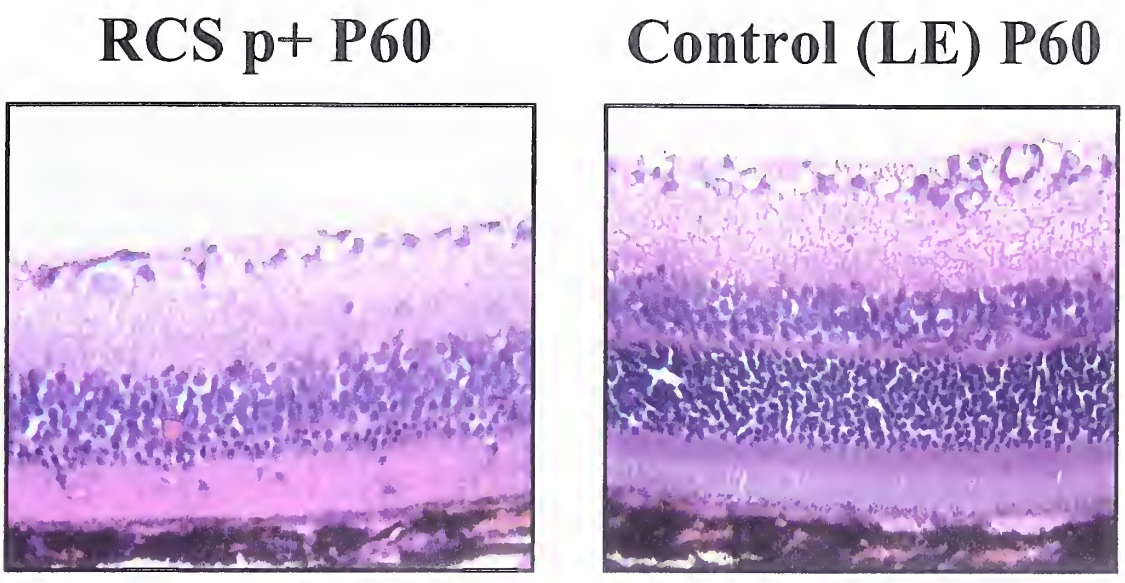

FIGURE 6. H&E sections of RCS p+ and Long-Evans control at postnatal date P60 showing the continued presence of a outer segment debris zone with marked thinning of the outer nuclear layer (ONL) as compared to the non-dystrophic control.

4Di-10ASP Dye and the RCS p+ animal

After injection of the fluorescent carbocyanine dye, 4Di-10ASP, into the superficial superior colliculus of newborn RCS p+ pups, all but two labeled pups survived the procedure and were subsequently not rejected by the mother post-operatively. Since the initial hypothesis stated that black-eyed, pigmented RCS p+ rats have delayed microglial migration to the photoreceptor layer, the first animal was sacrificed at P21 – a time period noted by Thanos et al to be the postnatal date at which microglial perikarya were visible within the PRL of pink-eyed RCS rats. Visualized under confocal microscopy for fluorescence, the first photomicrograph shows that microglia are visible in the ganglion cell layer (GCL), inner plexiform/inner nuclear layer (IPL/INL), and the outer plexiform layer (OPL). By this staining method based on retrograde axoplasmic transport of fluorescent dye from ganglion cell axons projections

to the superior colliculus, it is evident that no microglia have reached the PRL (Fig. 7). The linear band of fluorescence visible at the bottom of the image in the upper right is indicative of the autofluorescence of photoreceptor outer segments which contain lipofuscin.

Following the course of microglial migration, the P31 photomicrograph shows that these cells can be found in the ganglion cell layer (GCL), inner plexiform/inner nuclear layer (IPL/INL), outer plexiform layer (OPL), and also in the photoreceptor layer (Fig. 8). Images from the subsequent RCS p+ rats P45 and P60, again illustrate that microglia have reached the PRL, but are now visible in greater numbers (Fig. 9 and 10). Also visible is the increased autofluorescence as the outer segment debris continues to accumulate and is most heavily fluorescent in the P60 animal.

Indirect Immunohistochemical staining and the RCS p+ animal

In order to corroborate the results obtained from the superior colliculus injection (SCI) technique used to fluorescently label the RCS p+ animal, staining of the same strain was employed using primary antibodies to CD11b (OX42) and examined under confocal to visualize the secondary streptavidin -Texas Red antibody. The first image obtained from the RCS p+ P21 rat shows that OX42 positive cells are visible in the outer plexiform layer (Fig. 11). Additionally, the negative control for which PBS was used in place of the primary antibody, reveals no signal. Similar to the results obtained through the SCI method, the RCS p+ P31 section shows OX42 positive cells in the outer plexiform layer (OPL) and also within the photoreceptor layer (PRL) as well (Fig. 12). As in the prior section, the negative control shows no signal. Finally, visualization of the RCS p+ P45 section demonstrates OX42 positive cells exclusively within the

photoreceptor layer (PRL) with the negative control below it (Fig. 13). Note, as indicated with the sequential sections from the 4Di-10ASP labeled, there is a progressive thinning of the outer nuclear layer (ONL). Since the purpose of this study was to demonstrate the difference in timing of microglial migration between pigmented and non-pigmented RCS strains, sections of the P60 RCS p+ retina were not stained for OX42 positive cells.

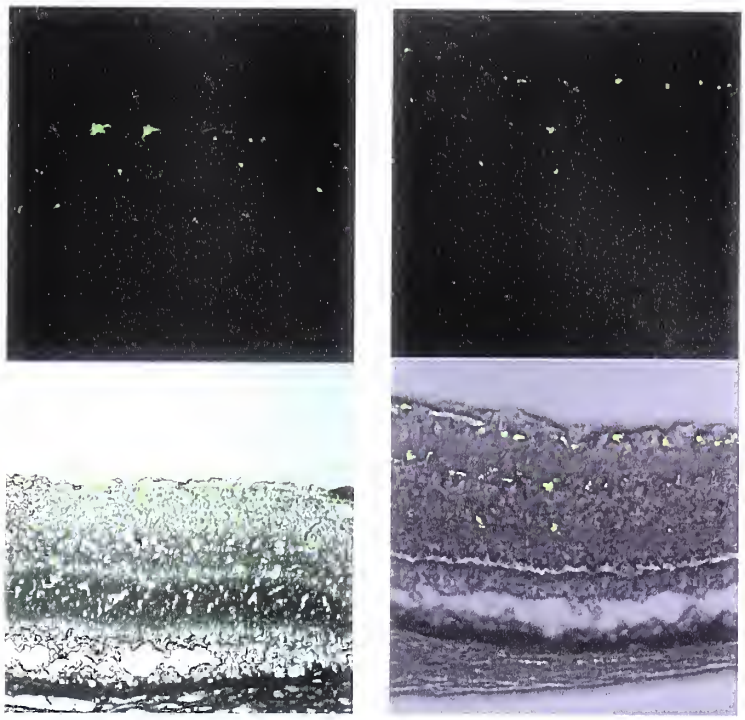

RCS p+ P21 (SCI)

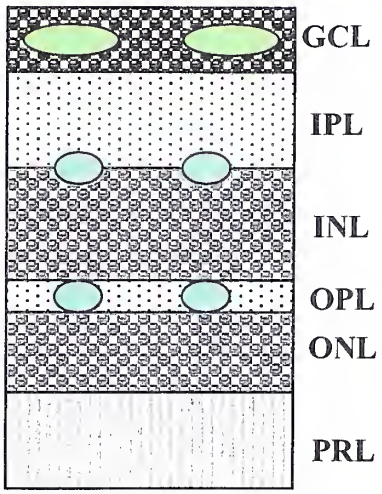

FIGURE 7. Labeling of retinal microglia using 4Di-10ASP as a superior colliculus injection (SCI). Fluorescence photomicrographs from the RCS p+ P21 rat indicate the presence of microglia in the ganglion cell layer (GCL), inner plexiform/inner nuclear layer (IPL/INL), the outer plexiform layer (OPL), but not in the photoreceptor layer (PRL) where mild debris has begun to accumulate.

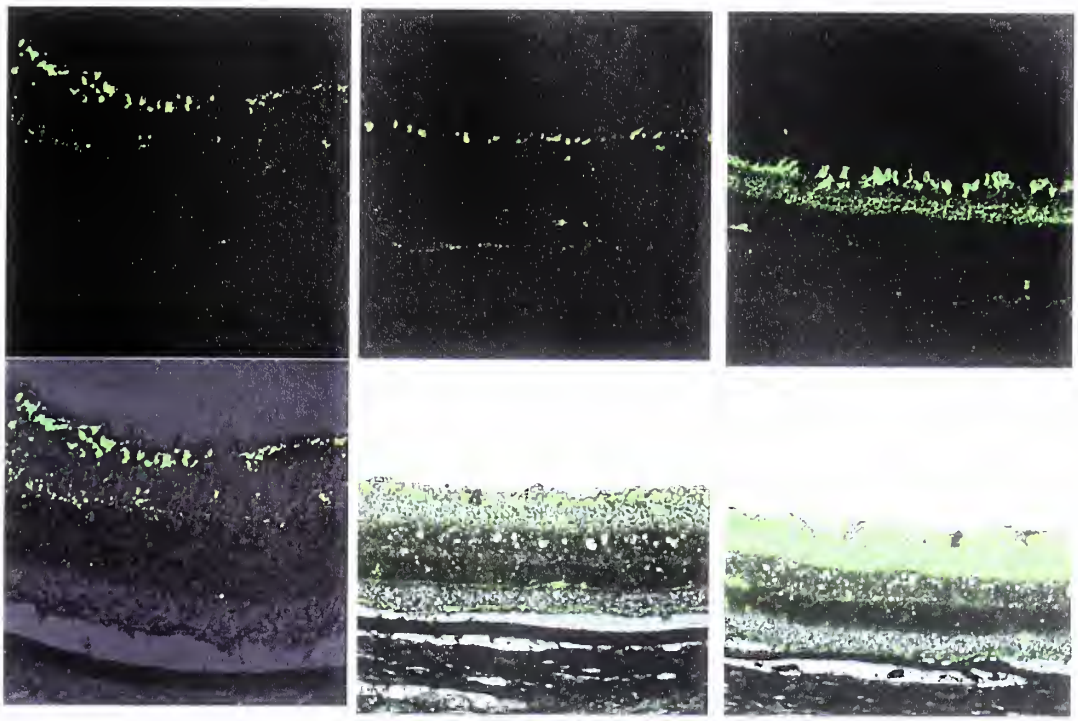

RCS p+ P31 (SCI)

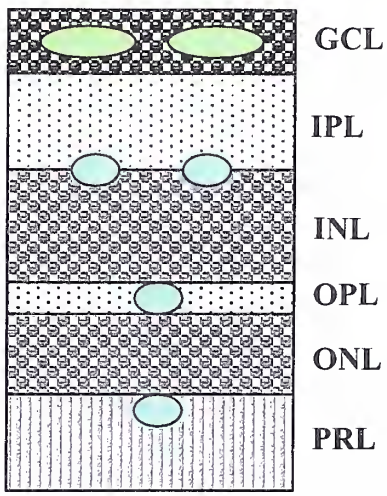

FIGURE 8. Labeling of retinal microglia using 4Di-10ASP as a superior colliculus injection (SCI). Fluorescence photomicrographs from the RCS p+ P31 rat show the presence of microglia in the ganglion cell layer (GCL), inner plexiform/inner nuclear layer (IPL/INL), outer plexiform layer (OPL), and the photoreceptor layer (PRL).

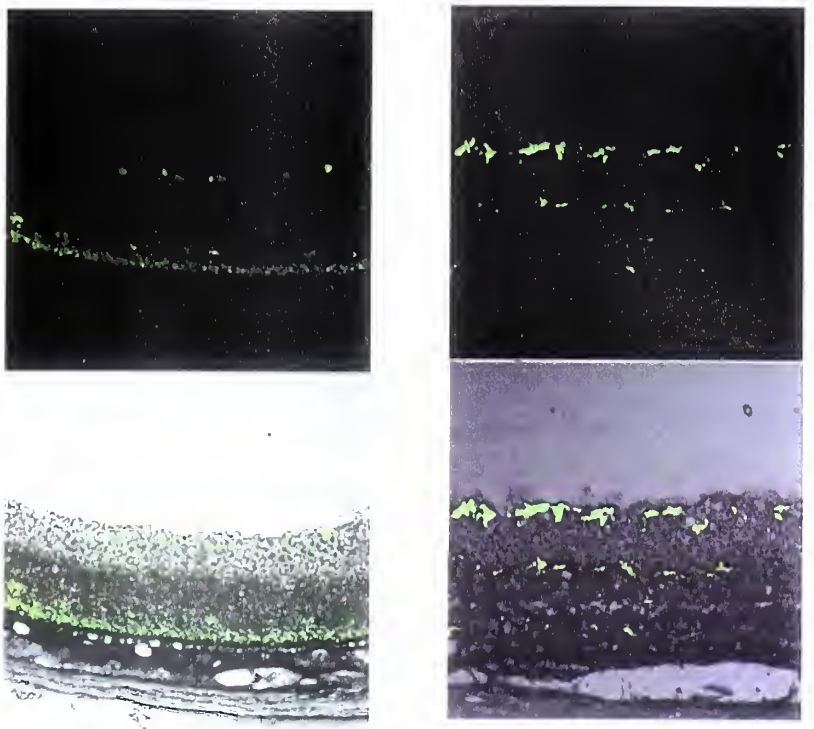

RCS p+ P45 (SCI)

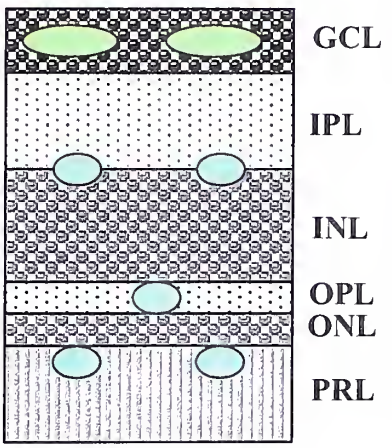

FIGURE 9. Labeling of retinal microglia using 4Di-10ASP as a superior colliculus injection (SCI). Fluorescence photomicrographs from the RCS p+ P45 rat show the presence of microglia in the ganglion cell layer (GCL), inner plexiform/inner nuclear layer (IPL/INL), outer plexiform layer (OPL), and the photoreceptor layer (PRL).

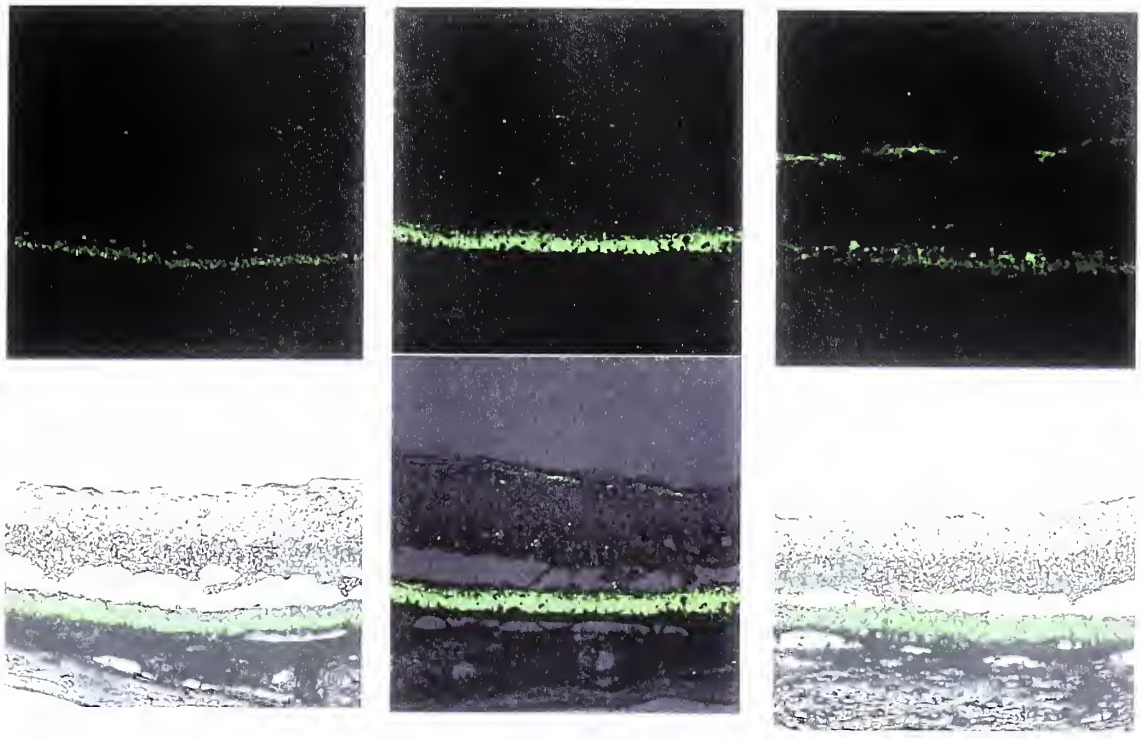

RCS p+ P60 (SCI)

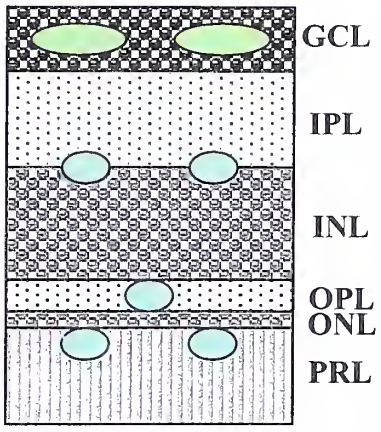

FIGURE 10. Labeling of retinal microglia using 4Di-10ASP as a superior colliculus injection (SCI). Fluorescence photomicrographs from the RCS p+ P60 rat show the presence of microglia in the ganglion cell layer (GCL), inner plexiform/inner nuclear layer (IPL/INL), outer plexiform layer (OPL), and the photoreceptor layer (PRL).

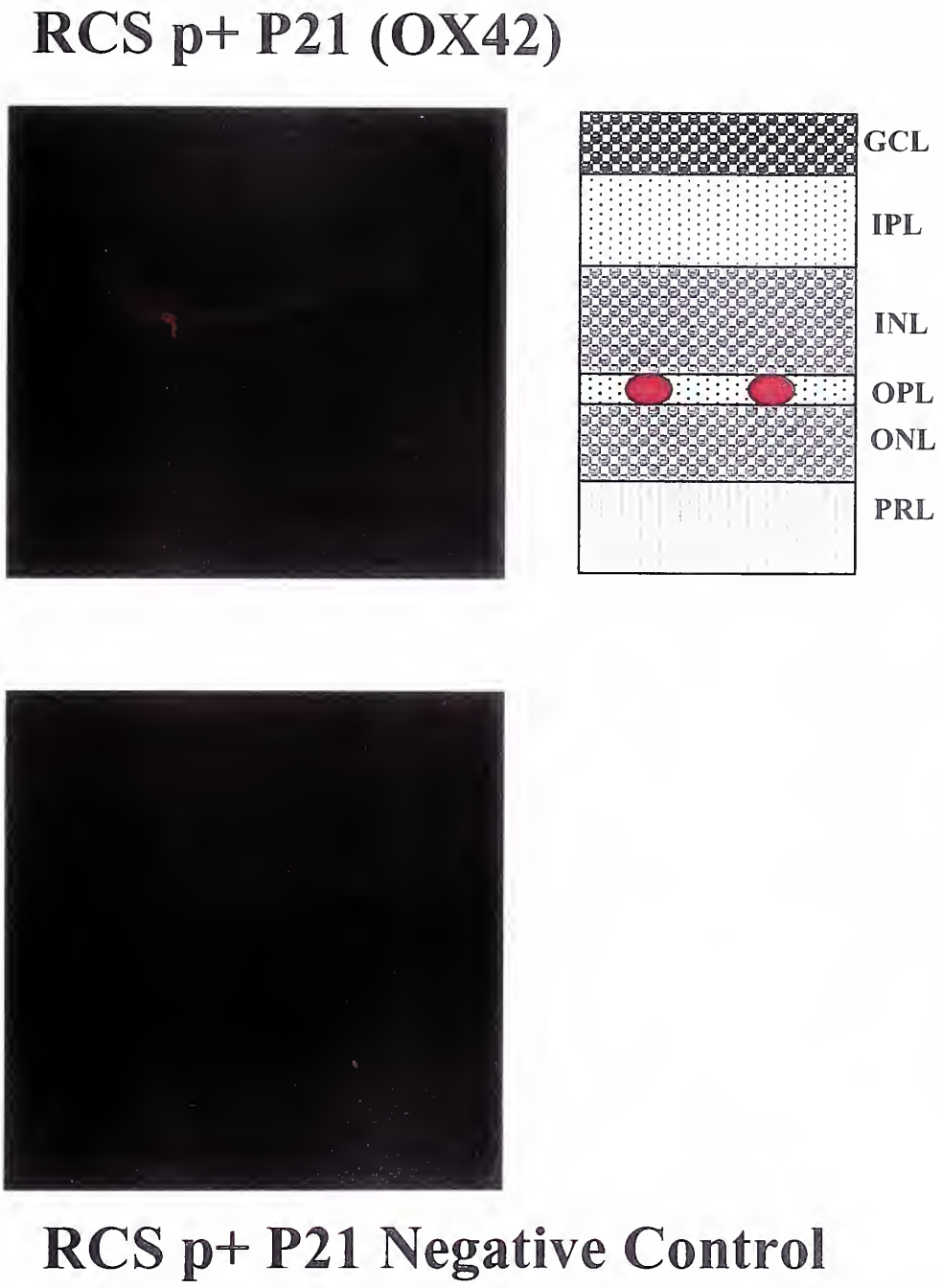

FIGURE 11. Labeling of retinal microglia in the RCS p+ rat postnatal day 21 via indirect immunohistochemistry using the antibody to CD 11b (OX42) demonstrates the presence of OX42 positive microglia in the outer plexiform layer (OPL). The image on the bottom shows the negative control.

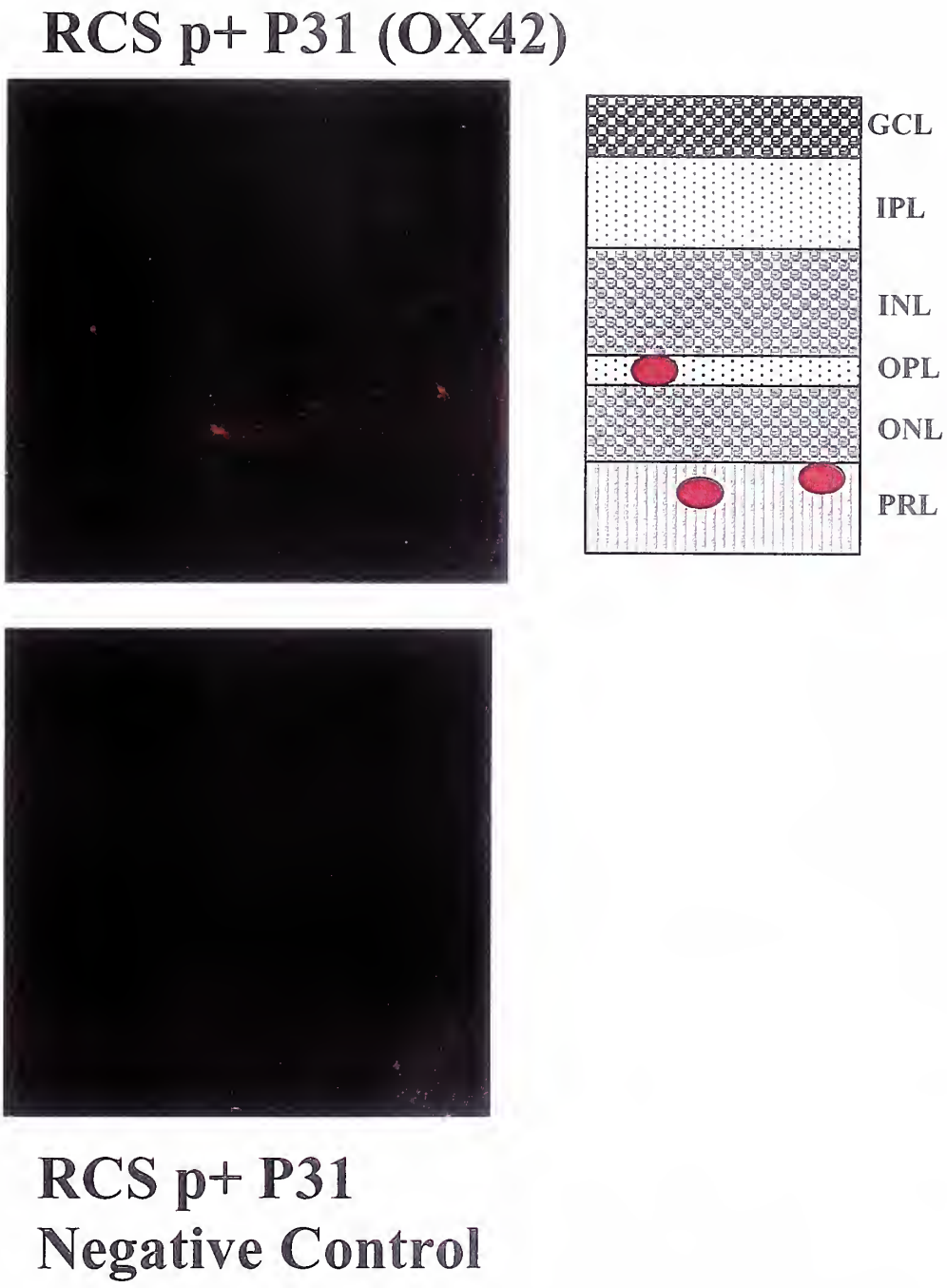

FIGURE 12. Labeling of retinal microglia in the RCS p+ rat postnatal day 31 via indirect immunohistochemistry using the antibody to CD 11b (OX42) demonstrates the presence of OX42 positive microglia in the outer plexiform layer (OPL) and photoreceptor layer (PRL). The image on the bottom shows the negative control.

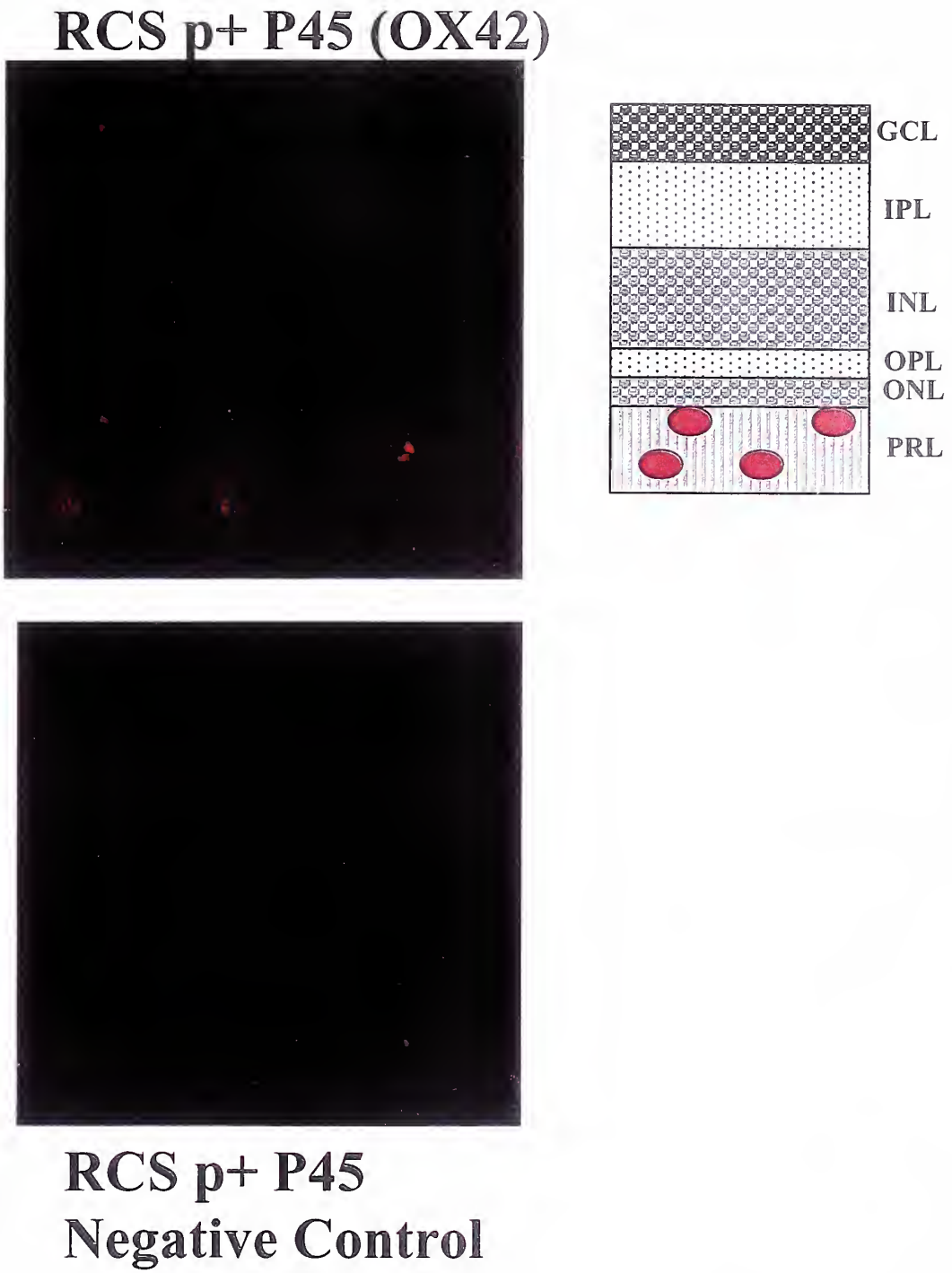

FIGURE 13. Labeling of retinal microglia in the RCS p+ rat postnatal day 45 via indirect immunohistochemistry using the antibody to CD 11b (OX42) demonstrates the presence of OX42 positive microglia entirely within the photoreceptor layer (PRL). The image on the bottom shows the negative control.

DISCUSSION

This experiment was designed to use different methodologies aimed at identifying retinal microglia to ascertain if there was a difference in the time course of microglial migration between two strains of rats with inherited retinal dystrophy. From prior studies, it has been shown that retinal microglia are attracted to the photoreceptor layer as photoreceptor outer segment debris accumulates. However, this study by Thanos et al made exclusive use of the pink-eyed RCS variant – a strain not as analogous to humans due its difference in pigmentation from its black-eyed cousin, the RCS p+ strain (28).

In comparing the photomicrographs from both the SCI-labeling method and OX42 staining, there is a pattern of similarity evident. A side-by-side comparison of the images in the RCS p+ variant shows that retinal microglia have not reached the photoreceptor layer (PRL) by P21 as in the pink-eyed RCS strain. It is only by postnatal day 31 that microglia are seen in the PRL using both methods. While it cannot be stated that microglia have first reached the PRL by P31, it can be stated that they do migrate differently in this pigmented strain since they have not reached the PRL by P21. An answer to the question of when microglia first arrive could certainly be answered through sectioning of RCS p+ animals from each day from P21 through P31. Unfortunately, that specific question cannot be addressed with the present data.

In addition to demonstrating a different timeline for microglial migration, this study also shows staining for OX42 positive cells can, in fact, be used to corroborate the results obtained from fluorescence labeling (SCI). Moreover, OX42 positive cells provide an excellent basis of comparison to the SCI method as there is less confounding with the autofluorescence evident in the latter technique. That both methodologies

provided nearly identical patterns of migration lends credence to their use in future studies of migration patterns of retinal microglia. Additionally, it should be noted that dual-staining (OX42 and SCI) was attempted using the frozen sections from the SCI RCS p+ pups. However, such attempts were met with a loss of coherent fluorescence and were subsequently abandoned in favor of the separate approach used in this study. Furthermore, after analysis of the OX42 positive stains, it is notable that only cells from the outer plexiform layer (OPL) and outwards are positive. No simple explanation exists for this finding since other studies involving microglial migration have consistently noted a microglial presence within the ganglion cell layer (GCL) despite migration (28).

While this experiment effectively concludes that a difference of ten days or less exists in microglial migration to the PRL in RCS p+ rats, it does not offer an explanation for this delay. Given the data from LaVail et al showing that pigmented RCS rats have slower rates of photoreceptor degeneration as compared to the pink-eyed variant, we hypothesized that microglial migration might also be delayed (16). Comparing the photomicrographs from LaVail et al of the pink-eyed RCS variant to our H&E stains, it is also evident that while the P21 section from the RCS p+ shows indications of some photoreceptor degeneration, it is not nearly as advanced as the P21 section from the pink-eyed RCS variant.

A potential limitation of this study's experimental design was that it did not control for light exposure and its potential impact on the rate of microglial migration. In a study by Streilein et al using an albino mouse model, they concluded that "acute light toxicity" in this non-pigmented mouse hastened the invasion of retinal microglia to the photoreceptor layer and the subretinal space adjacent to the RPE (33). However, they

also determined that the pigmented mouse variant which was used did not show any alteration in microglial migration with varying light exposure.

One crucial question remains to be answered: what causes retinal microglia to migrate to photoreceptor layer and what is their function once they reach their destination? Numerous studies have demonstrated that the administration of agents ranging from microglia-inhibiting factor (MIF, a tripeptide analogous to human IgG with receptors on monocytic cell lines) to calcium channel blockers (e.g., nilvadipine) have beneficial effects in the preservation of retinal morphology (9, 32). Yet, no study has definitively identified outer segment debris as the main chemotactic stimulus as is currently theorized.

As such, the rationale behind creating a reliable method for microglial isolation was two-fold – to create a population of cells to test the method of OX42 staining and to generate a technique to isolate retinal microglia in sufficient quantities to be able to perform an *in vitro* chemotaxis assay. Such a comparison of *in vivo* versus *in vitro* microglial chemotaxis could help to identify substances both chemotactic for microglia and chemoprotective for the retina.

REFERENCES

1. Dowling, J.E. and Sidman, R.L. 1962. Inherited retinal dystrophy in the rat. *J Cell Biol.*, 14: 73-109.
2. Pierce, E.A., 2001. Pathways to photoreceptor cell death in inherited retinal degerenations. *BioEssays* 23: 605-61.
3. Milam, A.H., Li, Z.Y., and Fariss, R.N. 1998. Histopathology of the human retina in retinitis pigmentosa. *Prog. Retina Eye Research* 17: 175-205.
4. Tso, M.O.M., Zhang, C., Abler, A.S., Chang, C.J., Wong F., Chang, G.Q. and Lam, T.T. 1994. Apoptosis leads to photoreceptor degeneration in inherited retinal dystrophy of RCS rats. *Invest. Ophthalmol. Vis. Sci.* 35: 2693-2699.
5. La Vail, M.M. 1981. Assignment of retinal dystrophy (RDY) to linkage group IV of the rat. *J. Hered.* 772: 294-296..
6. D'Cruz, P.M., Yasamura D., Weir J., Matthes, M., Abderrahim, H., LaVail, M.M., and Vollrath, D. 2000. Mutation of the receptor tyrosine kinase gene *Mertk* in the retinal dystrophic RCS rat. *Hum. Mol. Genet.* 9:645-651.
7. Gal, A., Li, Y., Thompson, D.A., Weir, J., Orth, U., Jacobson, S.G., Apfelstedt-Sylla, E. and Vollrath, D. 2000. Mutations in *MERTK*, the human orthologue of the RCS rat retinal dystrophy gene, cause retinitis pigmentosa. *Nat. Genet.* 26:270-271.
8. Faktorovich, E.G., Steinberg, R.H., Yasamura, D., Matthes, M.T. and LaVail, M.M. 1990. Photoreceptor degeneration in inherited retinal dystrophy delayed by the basic fibroblast growth factor. *Nature*. 347: 83-86.

9. Steinberg, R.H. 1994. Survival factors in retinal degenerations. *Curr. Opin. Neurobiol.* 4: 515-524.

10. Thanos, S. 1992. Sick photoreceptors attract activated microglia from the ganglion cell layer: a model to study the inflammatory cascades in rats with inherited retinal dystrophy. *Brain Res.* 588: 21-28.

11. Rao, N.A., Kimoto, T., Zamir, E., Giri, R., Want, R., Ito, S., Pararajasegaram, G., Read, R.W. and Wu, G-S. 2003. Pathogenetic Role of Retinal Microglia in Experimental Uveoretinitis. *Invest. Ophthalmol. Vis. Sci.* 44: 22-31.

12. Lee, Y.B., Nagai, A. and Kim, S.U. 2002. Cytokines, chemokines, and cytokine receptors in human microglia. *J. Neurosci. Res.* 69: 94-103

13. Penfold, P.L., Provis, J.M. and Liew, S.C. 1993. Human retinal microglia express phenotypic characteristics in common with dendritic antigen-presenting cells. *J. Neuroimmunol.* 45: 183-191.

14. Thanos, S., Moore, S. and Hong, Y. 1996. Retinal microglia. *Prog. Ret. Eye Res.* 15: 331-361.

15. Little, C.W., Castillo, B., DiLoreto, D.A., Cox, C., Wyatt, J., del Cerro, C, and del Cerro, M. 1996. Transplantation of Human Fetal Retinal Pigment Epithelium Rescues Photoreceptor Cells from Degeneration in the Royal College of Surgeons Rat Retina. *Invest. Ophthalmol. Vis. Sci.* 37: 204-211.

16. LaVail, M.M and Battelle, B-A. 1975. Influence of Eye Pigmentation and Light Deprivation on Inherited Retinal Dystrophy in the Rat. *Exp. Eye Res.* 21: 167-192.

17. Berson, E.L. 1971. Light deprivation for early retinitis pigmentosa. A Hypothesis. *Arch Ophthalmol.* 85: 521-529.

18. Bourne, M.C. and Grüneberg, H. 1939. Degeneration of the retina and cataract, a new recessive gene in the rat. *Brit J. Ophthalmol.* 22: 613-623.

19. Sidman, R.L. and Pearlstein, R. 1965. Pink-eyed dilution (p) gene in rodents: increased pigmentation in tissue culture. *Dev. Biol.*. 12: 93-116.

20. LaVail, M.M. 1981. Photoreceptor characteristics in congenic strains of RCS rats. *Invest. Ophthalmol. Vis. Sci.* 20: 671-675.

21. Nissl, F. 1904. Zur Histopathologie der paralytischen Rindenerkrankungen und gliösen Erscheinungen bei verscheidenen Psychosen. *Archs. Psych.* 32: 1-21.

22. Ramon y Cajal. 1929. Degeneration and regeneration of the nervous system (May, R.M., translation). University Press, London.

23. Theele, D.P. and Streit, W.J. 1993. A chronicle of microglial ontogeny. *Glia*. 7: 5-8.

24. Schnitzer, J. and Scherer, J. 1990. Microglia cell responses in the rabbit retina following transection of the optic nerve. *J. Comp. Neurol.* 302: 779-791.

25. Zhang, J., Wu, G-S., Ishimoto, S., Pararajasegaram, G., Rao, NA. 1997. Expression of Major Histocompatibility Complex Molecules in Roden Retina. *Invest. Ophthalmol. Vis. Sci.* 38: 1848-1857.

26. Roque, R.S., Imperial, C.J., Caldwell, R.B. 1996. Microglial cells invade the outer retina as photoreceptors degenerate in Royal College of Surgeons rat. *Invest. Ophthalmol. Vis. Sci.* 37: 196-203.

27. Jeffery, G. and Perry, V.H. 1982. Evidence for ganglion cell death during development of the ipsilateral retinal projection in the rat. *Devl. Brain Res.* 2: 176-180.

28. Thanos, S. and Richter, W. 1993. The migratory potential of vitally labelled microglial cells within the retina of rats with hereditary photoreceptor dystrophy. *J Devl Neuroscience*. 11: 671-680.

29. Becher, B., Antel J.P. 1996. Comparison of phenotypic and functional properties of immediately ex vivo cultured human adult microglia. *Glia* 18: 1-10.

30. Guillemin, G., Boussin, F.D., Criotoru, J., Frank-Duchenne, M., Le Grand, R., Lazarini, F., Dormont, D. 1997. Obtention and characterization of primary astrocyte and microglial cultures from adult monkey brains. *J. Neurosci. Res.* 49: 576-591.

31. De Groot, C.J.A., Montagne, L., Janssen, I., Ravid, R., Van Der Valk, P., Veerhuis, R. 2000. Isolation and characterization of adult microglial cells and oligodendrocytes derived from postmortem human brain tissue. *Brain Research Protocols*. 5: 85-94.

32. Yamakazi, H., Ohguro, H., Maeda, T., Maruyama, I., Takano, Y., Metoki, T., Nakazawa, M., Sawada, H., Dezawa, M. 2002. Preservation of retinal morphology and functions in royal college of surgeons rat by nilvadipine, a Ca(2+) antagonist. *Invest. Ophthalmol. Vis. Sci.* 43: 919-926.

33. Streilein, J.W., Ng, T.F. 2001. Light-induced migration of retinal microglia into the subretinal space. *Invest. Ophthalmol. Vis. Sci.* 42: 3301-3310.

HARVEY CUSHING/JOHN HAY WHITNEY MEDICAL LIBRARY

MANUSCRIPT THESES

Unpublished theses submitted for the Master's and Doctor's degrees and deposited in the Medical Library are to be used only with due regard to the rights of the authors. Bibliographical references may be noted, but passages must not be copied without permission of the authors, and without proper credit being given in subsequent written or published work.

This thesis by
has been used by the following person, whose signatures attest their acceptance of the above restrictions.

NAME AND ADDRESS **DATE**